

Temporo-Parietal Brain Network Impairment Is Related To EEG ALPHA3/ALPHA2 Frequency Power Ratio in Prodromal Alzheimer's Disease

Moretti D V*, Paternicò D, Binetti G, Zanetti O and Frisoni G B

IRCCS S. Giovanni di Dio Fatebenefratelli, Brescia, Italy

Abstract

Background: Reliable biomarkers are the new frontier for an early diagnosis of Alzheimer's disease and to monitor therapeutic options

Objective: Volume reduction in temporo-parietal network is associated to mild cognitive impairment (MCI) due to Alzheimer disease (AD). The increase of EEG alpha3/alpha2 ratio has been associated with AD-converter MCI subjects. We investigated the association of alpha3/alpha2 ratio with patterns of cortical thickness in MCI.

Methods: 74 adult subjects with MCI underwent clinical and neuropsychological evaluation, electroencephalogram (EEG) recording and high resolution 3D magnetic resonance imaging (MRI). Alpha3/alpha2 power ratio as well as cortical thickness was computed for each subject. Three MCI groups were detected according to increasing tertile values of alpha3/alpha2 and difference of cortical thickness among the groups estimated. Pearson's r was used to assess the topography of the correlation between cortical thinning and memory impairment.

Results: High a3/2 group had total cortical grey matter (CGM) volume reduction of 471 mm² than Low a3/a2 group ($p < .001$). High a3/2 group showed a similar but less marked pattern (160 mm²) of cortical thinning when compared to Middle a3/a2 group ($p < .001$). Moreover, high a3/2 group had wider cortical thinning than other groups, mapped to the Supramarginal and Precuneus bilaterally. No significant cortical thickness difference was found between Middle and Low a3/a2 groups.

Conclusion: High EEG alpha3/alpha2 ratio was associated with impairment of temporo-parietal cortical brain in MCI subjects. The combination of EEG alpha3/alpha2 power ratio and cortical thickness measure could be useful for identifying individuals at risk for progression to AD dementia and may be of value in clinical context.

Introduction

The identification and validation of biomarkers for diagnosing, monitoring progression and predicting onset of Alzheimer's disease (AD) has been a main focus of AD research in the past 10 years. In line with recently published research criteria, it is becoming clear that the integration of different biomarkers is a milestone for a correct and early diagnosis of mild cognitive impairment due to AD [1,2]. To date, the most studied and validated biomarkers are Aβ₄₂ and tau in the cerebrospinal fluid (CSF), glucose hypometabolism on fluorodeoxyglucose positron emission tomography (18F-FDG PET), atrophy of hippocampal volume (HV) on magnetic resonance (MR), and brain amyloid deposition on amyloid imaging with PET [3,4]. Anyway, some controversies remain to debate. The latter biomarkers have a good sensibility in identifying subjects with a neurodegenerative disorders at high risk to convert in dementia, but they lack a reliable specificity that allow a clear-cut diagnosis of the different subtypes of dementias. Of note, in neurodegenerative disorders, like AD or other dementias, the brain networks modifies many years before clinical manifestations. Recent MRI studies have demonstrated that a large neural network is altered in subjects with prodromal AD, including precuneus, medial temporal, parietal and frontal cortices [5-9]. In particular, subjects with cognitive decline have shown early atrophy and loss of grey matter in cortical specific brain areas [10,11], including hippocampal, medial temporal and parietal lobes. In the conceptual frame of the integration of biomarkers for an early and highly predictive diagnosis, the EEG could be a reliable tool [12]. Indeed, it is widely accepted that the cerebral EEG rhythms reflect the underlying brain network activity [13]. As a consequence, modifications in EEG rhythms could be an early sign of disease associated with AD-related structural and functional networks. Recently, it has been demonstrated that the increase of high alpha relative to low alpha power is a reliable

EEG marker of hippocampal atrophy and amigdalo-hippocampal complex atrophy [14,15]. Furthermore, the increase in alpha3/alpha2 power ratio has been demonstrated predictive of conversion of patients with MCI in AD, but not in non-AD dementia [16]. The same increase of alpha3/alpha2 power ratio was found to be correlated with hippocampal atrophy in subjects with AD [12]. Finally, a recent study have shown that MCI subjects with highest alpha3/alpha2 power ratio present a peculiar pattern of basal ganglia and thalamic atrophy, detected with voxel-based-morphometry (VBM) technique, as compared to MCI groups with middle and low alpha3/alpha 2 power ratio [12]. The present explorative study shares the same theoretical background. The aim of the study is to extend the relationship of the alpha3/alpha2 EEG power ratio to the study of cerebral cortex atrophy in subjects with MCI. Two principal reasons supports this aim: 1) the hippocampal complex is strongly connected with temporo-parietal cortex; 2) in AD due to MCI there is the presence of both hippocampal and brain cortical atrophy. The cortical thickness analysis may provide a more sensitive measure of pathology by computing the distance between the white matter surface and GM/CSF boundary over the

*Corresponding author: Vito Davide Moretti, MD, PhD, IRCCS Giovanni di Dio Fatebenefratelli, Brescia, Italy, Tel: +39 0303501597; Fax: +39 0303533513; E-mail: davide.moretti@afar.it

Received July 08, 2013; Accepted July 29, 2013; Published August 05, 2013

Citation: Moretti DV, Paternicò D, Binetti G, Zanetti O, Frisoni GB (2013) Temporo-Parietal Brain Network Impairment Is Related To EEG ALPHA3/ALPHA2 Power Ratio in Prodromal Alzheimer's Disease. J Neurol Neurophysiol 4: 160. doi:10.4172/2155-9562.1000160

Copyright: © 2013 Moretti DV, et al. This is an open-access article distributed under the terms of the Creative Commons Attribution License, which permits unrestricted use, distribution, and reproduction in any medium, provided the original author and source are credited.

entire cortex and allowing a precise matching of cortical anatomy between subjects. Moreover, increasing thinning in specific cortical areas is peculiar of AD and it could predict conversion from MCI state to AD dementia [16].

As a consequence, the working hypothesis of the present study is that an increase in alpha3/alpha2 EEG power ratio would like to be associated with brain atrophy in temporo-parietal brain networks. Upper alpha synchronization could be explained in the frame of two recent neurophysiological theories: the inhibition timing hypothesis and the entropy's theory. As about the inhibition timing hypothesis, recent research [17-19] has shown that the upper alpha increase in power (or synchronization) is associated with an impairment of the transmission of semantic information thus preventing the semantic encoding necessary for memory formation. In the same conceptual frame, the entropy's theory state that synchronization is disadvantageous for storing information, as it reduces the flexibility of the system and the flow of information [20].

To the best of our knowledge, an approach considering the regional pattern of cortical atrophy in combination with the EEG markers was never be investigated. This is the first study investigating the pattern of cortical thickness in a population of MCI subjects with increasing levels of alpha3/alpha2 ratios. Results show that subjects with higher a3/a2 ratios when compared to subjects with lower and middle a3/a2 ratios showed significant and wide thinning both of global cortical volume and specific brain areas, like the Supramarginal gyrus and Precuneus bilaterally. Other smaller regions of cortical thinning were localized on the right hemisphere in the Insula, Parietal and Temporal cortex.

Materials and Methods

Subjects

For the present study, 74 subjects with MCI were recruited from the memory Clinic of the Scientific Institute for Research and Care (IRCCS) of Alzheimer's and psychiatric diseases 'Fatebenefratelli' in Brescia, Italy. All experimental protocols had been approved by the local ethics committee. Informed consent was obtained from all participants or their caregivers, according to the Code of Ethics of the World Medical Association (Declaration of Helsinki).

Diagnostic criteria

Patients were selected from a prospective study on the natural history of cognitive impairment (the translational outpatient memory clinic—TOMC study) carried out in the outpatient facility of the National Institute for the Research and Care of Alzheimer's Disease (IRCCS Istituto Centro San Giovanni di Dio Fatebenefratelli, Brescia, Italy).

The project was aimed to study the natural history of non-demented persons with apparently primary cognitive deficits, i.e., deficits not due to psychic (anxiety, depression, etc.) or physical (hypothyroidism, vitamin B12 and folate deficiency, uncontrolled heart disease, uncontrolled conditions (diabetes, etc.) in the absence of functional impairment. The selection criteria have the aim to include as much as possible primary prodromal dementia due to neurodegenerative disorders. Demographic and cognitive features of the subjects in study are summarized in Table 1.

Patients were rated with a series of standardized diagnostic and severity instruments, including the Mini-Mental State Examination (MMSE; [21] 5), the Clinical Dementia Rating Scale (CDRS; [22]), the

Hachinski Ischemic Scale (HIS; [23]) and the Instrumental and Basic Activities of Daily Living (IADL, BADL; [24]). In addition, patients underwent diagnostic neuroimaging procedures (magnetic resonance imaging, MRI), and laboratory testing to rule out other causes of cognitive impairment. These inclusion and exclusion criteria for MCI were based on previous seminal studies [25-27]. Inclusion criteria of the study were all of the following: (i) complaint by the patient, or report by a relative or the general practitioner, of memory or other cognitive disturbances; (ii) Mini-Mental State Examination (MMSE) score of 24–27/30, or MMSE of 28 and higher plus low performance (score of 2–6 or higher) on the clock drawing test [28]; (iii) sparing of instrumental and basic activities of daily living or functional impairment steadily due to causes other than cognitive impairment, such as physical impairments, sensory loss, gait or balance disturbances, etc. Exclusion criteria were any one of the following: (i) patients aged 90 years and older (no minimum age to participate in the study); (ii) history of depression (from mild to moderate or major depression) or juvenile-onset psychosis; (iii) history or neurological signs of major stroke; (iv) other psychiatric diseases, overt dementia, epilepsy, drug addiction, alcohol dependence; (v) use of psychoactive drugs, including acetylcholinesterase inhibitors or other drugs enhancing brain cognitive functions or biasing EEG activity; and (vi) current or previous uncontrolled or complicated systemic diseases (including diabetes mellitus), or traumatic brain injuries. All subjects were right-handed.

All patients underwent: (i) semi-structured interview with the patient and – whenever possible – with another informant (usually, the patient's spouse or a child of the patient) by a geriatrician or neurologist; (ii) physical and neurological examinations; (iii) performance-based tests of physical function, gait and balance; (iv) neuropsychological battery assessing memory (Babcock Story Recall – Rey–Osterrieth Complex Figure, Recall – Auditory-Verbal Learning Test, immediate and delayed recall; [28]) verbal and non-verbal memory, attention and executive functions (Trail Making Test B, A and B-A; Inverted Motor Learning-Clock Drawing Test; [28]), abstract reasoning thinking (Raven Colored Progressive Matrices; [28]), frontal functions (Inverted Motor Learning); language (Phonological and Semantic fluency-Token test, [28]), and apraxia and visuo-constructional abilities (Rey–Osterrieth Complex Figure, Rey figure copy, Clock Drawing Test; [28]); (v) assessment of depressive symptoms by means of the Center for Epidemiologic Studies Depression Scale (CES-D; [29]). All the neuropsychological tests were standardized on Italian population, thus

	Alpha3/Alpha2			
	High	Middle	Low	p
Demographic and clinical features				
Number of subjects	18	38	18	---
Age, years	70.4 ± 6.7 [60-85]	68.4 ± 8.2 [52-83]	70.4 ± 7.4 [57-80]	.55
Sex, female	13 (%)	24 (%)	14 (%)	.51
Education, years	6.6 ± 3.6 [4-18]	7.6 ± 3.7 [3-17]	8.3 ± 4.7 [3-18]	.42
Mini Mental State Exam	27 ± 1.7 [23-29]	27.4 ± 1.3 [24-30]	26.9 ± 1.2 [23-30]	.46
WMHs (mm ³)	2.78 ± 2.58	5.59 ± 6.60	2.57 ± 2.76	.09
Alpha3/alpha2	1.29 ± 0.1 [1.17-1.52]	1.08 ± 0.0 [1-1.16]	0.9 ± 0.1 [0.77-0.98]	.000

Table 1: Demographic and cognitive characteristics in the whole sample, disaggregated for increased levels of Alpha3/ Alpha2 Numbers denote mean ± standard deviation, number and [range]. p denotes significance on ANOVA.

scores were compared to normative values with age, education and gender corrections in an Italian population.

As the aim of our study was to evaluate the relationship between GM loss and alpha2/alpha3 ratios in MCI subjects, we did not consider the clinical subtype of MCI, i.e., amnesic, or non-amnesic, single or multiple domains.

EEG recordings

The EEG activity was recorded continuously from 19 sites by using electrodes set in an elastic cap (Electro-Cap International, Inc.) and positioned according to the 10–20 international systems (Fp1, Fp2, F7, F3, Fz, F4, F8, T3, C3, Cz, C4, T4, T5, P3, Pz, P4, T6, O1, and O2). In order to keep constant the level of vigilance, an operator controlled on-line the subject and the EEG traces, alerting the subject any time there were signs of behavioural and/or EEG drowsiness. The ground electrode was placed in front of Fz. The left and right mastoids served as reference for all electrodes. The recordings were used off-line to re-reference the scalp recordings to the common average. Re-referencing was done prior to the EEG artifact detection and analysis. Data were recorded with a band-pass filter of 0.3–70 Hz, and digitized at a sampling rate of 250 Hz (BrainAmp, BrainProducts, Germany). Electrodes-skin impedance was set below 5 kHz. Horizontal and vertical eye movements were detected by recording the electrooculogram (EOG). The recording lasted 5 min, with subjects with closed eyes. Longer recordings would have reduced the variability of the data, but they would also have increased the possibility of slowing of EEG oscillations due to reduced vigilance and arousal. EEG data were then analyzed and fragmented off-line in consecutive epochs of 2 s, with a frequency resolution of 0.5 Hz. The average number of epochs analyzed was 140, ranging from 130 to 150. The EEG epochs with ocular, muscular and other types of artifact were preliminary identified by a computerized automatic procedure [30]. Two expert electroencephalographers manually double-checked and confirmed the automatic selections. The epochs with ocular, muscular and other types of artifacts were discarded

Analysis of individual frequency bands

All recordings were obtained in the morning with subjects resting comfortably. Vigilance was continuously monitored in order to avoid drowsiness. A digital FFT-based power spectrum analysis (Welch technique, Hanning windowing function, no phase shift) computed – ranging from 2 to 45 Hz – the power density of EEG rhythms with a 0.5 Hz frequency resolution. Two anchor frequencies were selected according to the literature guidelines [31,32], that is, the theta/alpha transition frequency (TF) and the individual alpha frequency (IAF) peak. These anchor frequencies were computed on the power spectra averaged across all recording electrodes. The TF marks the transition frequency between the theta and alpha bands, and represents an estimate of the frequency at which the theta and alpha spectra intersect. TF was computed as the minimum power in the alpha frequency range, since our EEG recordings were performed at rest. The IAF represents the frequency with the maximum power peak within the extended alpha range (5–14 Hz). Based on TF and IAF, we estimated the frequency band range for each subject, as follows: delta from TF-4 to TF- 2, theta from TF-2 to TF, low alpha band (alpha1 and alpha2) from TF to IAF, and high alpha band (or alpha3) from IAF to IAF + 2. The alpha1 and alpha2 bands were computed for each subject as follows: alpha1 from TF to the middle point of the TF-IAF range, and alpha2 from such middle point to the IAF peak [12,13,32-34]. Moreover, within theta frequency the frequency peak (individual theta frequency, ITF) was also individuated. The mean frequency range

computed in MCI subjects considered as a whole are: delta 2.9–4.9 Hz; theta 4.9–6.9 Hz; alpha1 6.9–8.9 Hz; alpha2 8.9–10.9 Hz; alpha3 10.9–12.9 Hz; . Finally, in the frequency bands determined on an individual basis, we computed the relative power spectra for each subject. The relative power density for each frequency band was computed as the ratio between the absolute power and the mean power spectra from 2 to 45 Hz. The relative band power at each band was defined as the mean of the relative band power for each frequency bin within that band. The alpha3/alpha2 was computed in all subjects and three groups were obtained according to increasing tertiles values of alpha3/alpha2: low ($a3/a2 < 1$); middle ($1 < a3/a2 < 1.16$) and high ($a3/a2 > 1.17$). The three groups of MCI have been demonstrated in previous studies to be different in nature. In particular, the high alpha3/alpha 2 EEG power ratio MCI group is at major risk to convert to Alzheimer's disease [35], as well as to have different pattern of hippocampal atrophy [36] and basal ganglia and thalamus gray matter lesions [12,13] as compared to the other alpha3/alpha2 power ratio MCI groups. Moreover, this group subdivision has been chosen for reason of homogeneity and comparability with the previous studies

MRI scans

For each subject, a high-resolution sagittal T1 weighted volumetric MR scan was acquired at the Neuroradiology Unit of the 'Citta' di Brescia' Hospital, Brescia, by using a 1.0 T Philips Gyroscan scanner, with a gradient echo 3D technique: TR=20 ms, TE=5 ms, flip angle=30, field of view=220 mm, acquisition matrix 256 · 256, slice thickness 1.3 mm.

Cortical thickness estimation steps

Cortical thickness measurements for 74 MCI patients were made using a fully automated magnetic resonance imaging-based analysis technique: FreeSurfer, a set of software tools for the study of cortical and subcortical anatomy. Briefly, in the cortical surface stream, the models of the boundary between white matter and cortical gray matter as well as the pial surface were constructed. Once these surfaces are known, an array of anatomical measures becomes possible, including: cortical thickness, surface area, curvature, and surface normal at each point on the cortex. In addition, a cortical surface-based atlas has been defined based on average folding patterns mapped to a sphere and surfaces from individuals can be aligned with this atlas with a high-dimensional nonlinear registration algorithm. The surface-based pipeline consists of several stages previous described in detail [35,36].

Single subject analysis: For each subjects the T1-weighted, anatomical 3-D MRI dataset were converted from Dicom format into .mgz format, then intensity variations are corrected and a normalized intensity image is created. The volume is registered with the Talairach atlas through an affine registration. Next, the skull is stripped using a deformable template model [37] and extracerebral voxels are removed. The intensity normalized, skull-stripped image is then operated on by a segmentation procedure based on the geometric structure of the gray-white interface. Voxels are classified as white or grey matter, cutting planes are chosen to separate the hemispheres from each other. A white matter surface is then generated for each hemisphere by tiling the outside of the white matter mass for that hemisphere. This initial surface is then refined to follow the intensity gradients between the white and gray matter. The white surface is then nudged to follow the intensity gradients between the gray matter and CSF, obtaining the pial surface. Cortical thickness measurements were obtained by calculating the distance between those surfaces (white and pial surface) at each

of approximately 160,000 points per hemisphere across the cortical mantle [38].

Group analysis: In order to relate and compare anatomical features across subjects, it is necessary to establish a mapping that specifies a unique correspondence between each location in one brain and the corresponding location in another. Thus, the pial surface of an individual subject is inflated to determine the large-scale folding patterns of the cortex and subsequently transformed into a sphere to minimize metric distortion. The folding patterns of the individual are then aligned with an average folding pattern using a high-resolution surface-based averaging. Thickness measures were mapped to the inflated surface of each participant's brain reconstruction allowing visualization of data across the entire cortical surface. Finally, cortical thickness was smoothed with a 20-mm full width at half height Gaussian kernel to reduce local variations in the measurements for further analysis.

Test-retest reproducibility of cortical thickness analysis

Previous studies have been investigated the reliability of the cortical thickness measurements: some of these addressed the effect of scanner-specific parameters, including field strength, pulse sequence, scanner upgrade, and vendor. The use of a different pulse sequence had a larger impact, as did different parameters employed in data processing. The within-scanner variability of global cortical thickness measurements reported in previous studies was 0.03-0.07 in average [39-42]. Scanner upgrade did not increase variability nor introduce bias while measurements across field strength were slightly biased (thicker at 3 T). In the study by Han et al the variability was 0.15 mm and 0.17 mm in average, respectively, for cross-scanner (Siemens/GE) and cross-field strength (1.5 T/3 T) comparisons. The recent study by Gronenshil et al also investigated the effects of data processing conditions such as Free Surfer version, workstation, and Macintosh operating system version. The authors reported significant differences between Free Surfer version (average: 2.8-3%) and a smaller differences between workstation and operating system version. On the whole, the results suggest that MRI-derived cortical thickness measures are highly reliable, however it is important to keep consistent the MRI parameters and data processing factors within any given structural neuroimaging study.

White matter hyperintensities (WMHs) computation

WMHs segmentation was performed on the FLAIR sequences using previously described algorithms [38]. Briefly, the procedure includes (i) filtering of FLAIR images to exclude radiofrequency inhomogeneities; (ii) segmentation of brain tissue from cerebrospinal fluid; (iii) modelling of brain intensity histogram as a Gaussian distribution; and (iv) classification of the voxels whose intensities were 3.5 standard deviations (SDs) above the mean as WMHs. In order to place each subject's WMHs map onto a common template, a set of linear and nonlinear transformations were applied with the protocol described below. FLAIR images were coregistered to the high resolution T1 image using a 9-parameters affine transformation (i.e., including rotation, translation and scaling) and the same alignment parameters were applied to the WMHs mask image created at the previous step. T1 images were intensity corrected in order to reduce adverse impact of the WMH voxel values on the accuracy of the nonlinear warping algorithm. This step involved estimating the normal white matter mean intensities surrounding the voxels classified as WMHs and replacing voxels in the T1 image corresponding to WMHs by the estimated values. T1 intensity-corrected images were normalized onto a standard

template by mean of high-dimensional cubic B-spline warp [39]. The template image used in this study was created from the MRI scans of a population of elderly subjects with a mix of diagnosis (AD, MCI, and normal) and was defined as the one that minimize the amount of distortion necessary to non-linearly align each subject MRI of the population. The parameters computed from nonlinear warping were then used to wrap each subject's FLAIR image and WMHs mask onto the template [40]. At the end of the process, anatomical regions are accurately matched between subjects, and WMHs voxels are in locations analogous to their original locations in the subjects' image. Total vascular load was then computed for each subject by counting the number of voxels segmented as WMHs and multiplying by voxel size (1.44 mm³). The WMHs were computed only to exclude significant differences in the cerebrovascular load in MCI groups and to avoid confounding variables in the statistical analysis. Of note, it has been demonstrated that the vascular load could bias the brain rhythms computation [12,13,41-44].

Statistical analysis

Differences between groups in sociodemographic and neuropsychological features were analyzed using SPSS version 13.0 (SPSS, Chicago, IL) performing an analysis of variance (ANOVA) for continuous variables and paired χ^2 test for dichotomous variables. For continuous variables, post-hoc pair wise comparisons among groups were performed with the Games-Howell or Bonferroni tests depending on homogeneity of variance tested with Levene's test.

Concerning the neuroimaging analysis, the Qdec interface in Free surfer software was used: a vertex-by-vertex analysis was carried out performing a general linear model to analyse whether any difference in mean cortical thickness existed between groups (low: $a_3/a_2 < 1 \mu V^2$; middle: $1 < a_3/a_2 < 1.16 \mu V^2$; high: $a_3/a_2 > 1.17 \mu V^2$). The following comparisons were carried out: High versus Low, High vs Middle and Middle vs Low. Age, sex, education, global cognitive level (MMSE score) and WMHs were introduced as covariates in the analysis to avoid confounding factors. Our results did not survived at $p < 0.05$ corrected, so we choose to apply an uncorrected but more restrictive significance threshold than 0.05 ($p \leq .001$) and we considered as significant only the clusters which also were wide equal or major to 30 mm². Finally a surface map was generated to display the results on an average brain. For illustrative purpose significance was set to a P-value of < 0.01 uncorrected for multiple comparisons

Results

Table 1 shows the sociodemographic and neuropsychological characteristics of MCI subgroups defined by the tertile values of alpha3/alpha2. The ANOVA analysis showed that there was not statistically significant differences between groups which resulted well paired for age, sex, white matter hyperintensities (WMHs) burden, education and global cognitive level. Anyway, age, sex, education, global cognitive level (MMSE score) and WMHs were introduced as covariates in the subsequent analysis to avoid confounding factors. Alpha3/alpha2 ratio levels were significant at Games-Howell post hoc comparisons ($p=0.000$).

Pattern of cortical thickness between groups

High vs Low: When compared to subjects with low a_3/a_2 ratios, patients with high a_3/a_2 ratio show thinning in the bilateral Spatiotemporal, Supramarginal and Precuneus cortex, in the right Inferior Parietal and Insula. The total CGM reduction in *High* a_3/a_2 group than *Low* a_3/a_2 group was 471 mm² (Figure 1 and Table 2).

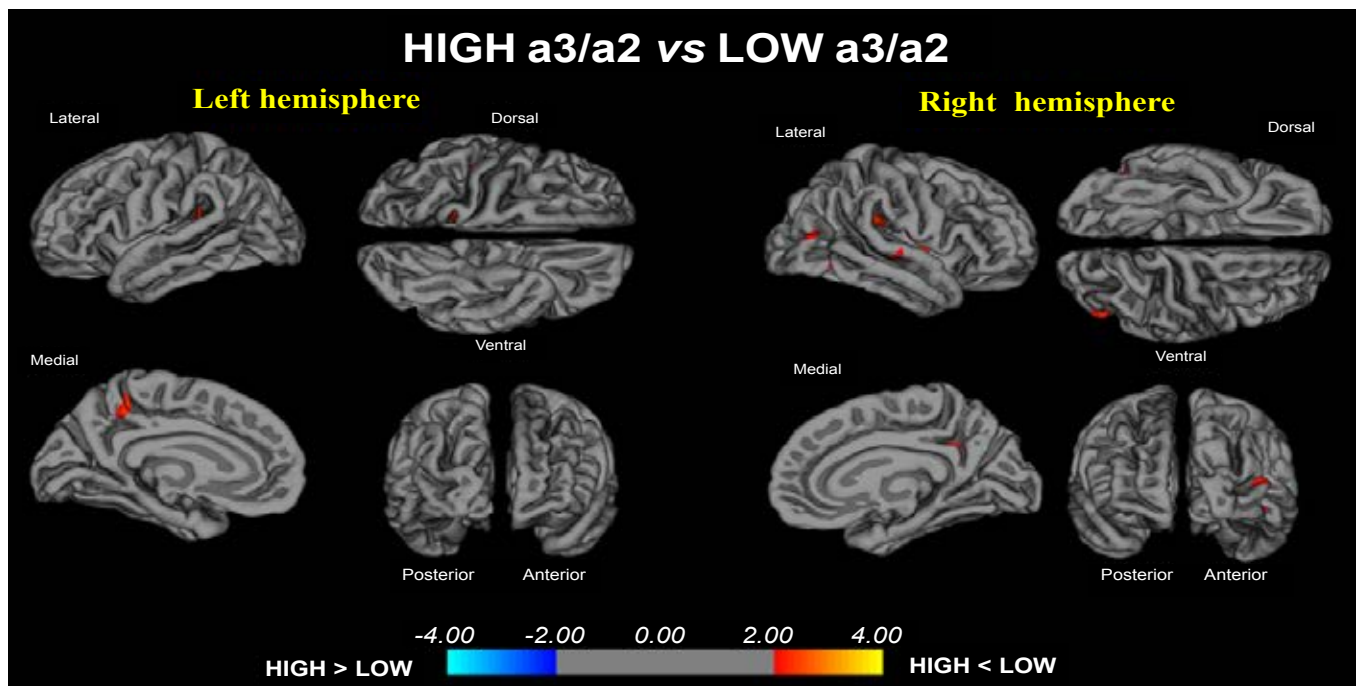


Figure 1: Brain regions with significant regional cortical thickness differences in MCI with high a3/a2 ratio compared to MCI with low a3/a2 ratio ($p < 0.01$ uncorrected). The colour-coding for p values is on a logarithmic scale. Warmer colour represents cortical thinning, cooler colour represents cortical thickening. Results are presented on the pial cortical surface of brain: dark gray regions represent sulci and light gray regions represent gyri.

HIGHa3/a2<LOW a3/a2								
CLUSTER SIZE(mm ²)	REGION	SIDE	STEREOTAXIC COORDIATE			P	THICKNESS(mm ²)	
			X	Y	Z		HIGH	LOW
61	Superior Temporal	L	-47	-36	9	<0.0001	2.25±0.15	2.00±0.18
60	Supramarginal	L	-40	-36	18	0.0008	1.95±0.18	2.08±0.19
35	Precuneus	L	-14	-48	58	0.0002	1.87±0.14	1.98±0.19
58	Superior Temporal	R	61	-22	-1	<0.0001	2.18±0.17	2.24±0.24
59	Supramarginal	R	49	-29	27	<0.0001	1.94±0.18	2.08±0.20
52	Precuneus	R	11	-49	30	0.0001	1.81±0.17	1.93±0.15
85	Inferior parietal	R	46	-75	10	0.0001	1.94±0.22	2.07±0.23
61	Insula	R	38	-2	3	0.0002	2.37±0.28	2.57±0.36
HIGHa3/a2<MIDDLE a3/a2								
CLUSTER SIZE(mm ²)	REGION	SIDE	STEREOTAXIC COORDIATE			P	THICKNESS(mm ²)	
			X	Y	Z		HIGH	MIDDLE
59	Post central	L	-57	-18	18	0.0002	1.51±0.15	1.62±0.17
71	Supramarginal	L	-53	-42	46	0.001	1.95±0.18	2.11±0.23
33	Precuneus	L	-16	-43	60	0.001	1.87±0.14	1.94±0.17

Table 2: Brain regions with significant regional cortical thickness differences in MCI with high a3/a2 ratio compared to MCI with low a3/a2 ratio (HIGH a3/a2 < LOW a3/a2) and MCI with middle a3/a2 ratio (HIGH a3/a2 < MIDDLE a3/a2). Cluster size represents the extension of contiguous significant voxels in the cluster obtained at $p < 0.01$ uncorrected (cluster size > 30 mm²). Stereotaxic coordinates reveal the position of the most significant voxel of the cluster, and side denotes its localization on the left (L) or right (R) brain hemisphere. Thickness denotes the average cortical thickness and standard deviation values within the cluster in high and middle a3/a2 groups. P denotes the significance level of the differences in thickness between groups.

High vs. Middle: The same group showed a similar but less wide pattern of cortical thinning when compared to middle a3/a2 group: the regions of atrophy were located in the left Supramarginal gyrus, left Precuneus and Postcentral cortex. The total CGM reduction in High a3/2 group than Middle a3/a2 group was 160 mm² (Figure 2, Table 2). When High group was compared to Low group the total extension of cortical thinning (471 mm²) was 34% wider than the other comparison in which High group was compared to Middle group (160 mm²). No regions of major cortical atrophy was found in groups with Middle or Low a3/a2 power ratio when compared to High a3/a2 group. No

significant cortical thickness differences were found between Middle and Low a3/a2 groups.

Discussion

The MCI concept

The concept of MCI has been evolving in the last years as much as the interest of scientific community has focused on the subjects that could develop AD. The previous concept of amnesic MCI has been turned in MCI due to AD, according to recent recommendations [2].

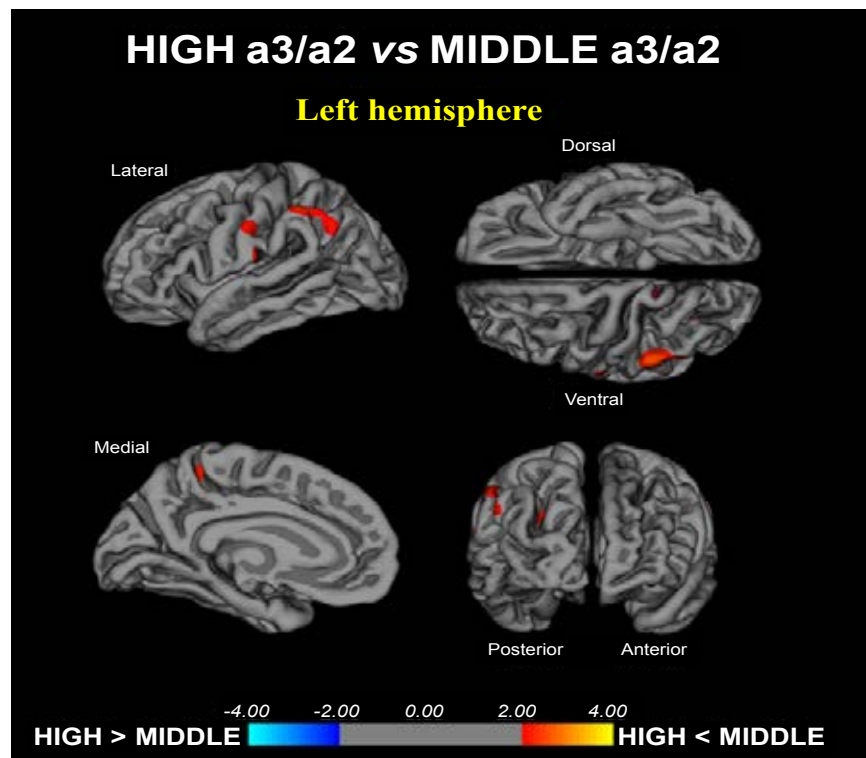


Figure 2: Brain regions with significant regional cortical thickness differences in MCI with high a3/a2 ratio compared to MCI with middle a3/a2 ratio ($p < 0.01$ uncorrected). The colour-coding for p values is on a logarithmic scale. Warmer colour represents cortical thinning, cooler colour represents cortical thickening. Results are presented on the pial cortical surface of brain: dark gray regions represent sulci and light gray regions represent gyri.

The most important novelty of these new diagnostic criteria is the recognized need of reliable biomarkers associated to the judgment of a clinician for the early diagnosis of subjects that are at major risk to develop AD. Nevertheless, different etiologies in addition to AD pathophysiological process may coexist in an individual who meets the criteria for MCI due to AD [45]. Of note, these criteria assume that it is possible to identify those individuals with AD pathophysiological process as the likely primary cause of their progressive cognitive dysfunction. Moreover, it is important to note that, as AD is a slow, progressive disorder, with no fixed events that define its onset, it is particularly challenging for clinicians to identify transition points for individual patients. Thus, it is difficult to identify the point at which the transition from the asymptomatic to the symptomatic prodementia phase [46], or from the symptomatic prodementia phase to dementia onset, occurs [47]. Moreover, there is greater diagnostic uncertainty earlier in the disease process. This issue is confirmed by a recent study [48] that found a group of MCI subjects who had only abnormal A beta 42 with no evidence of neuronal injury. According to the AD biomarker dynamic model and the above-mentioned guidelines, those subjects should not have shown cognitive symptoms, as clinical symptom severity correlates with neuronal injury rather than beta-amyloid deposition. The authors hypothesized that they could have had neurodegenerative biomarkers very near to the threshold for abnormality but not sufficiently high enough to indicate the presence of neuronal injury. Limitation intrinsic to the use of fixed cut-offs could explain these findings. These findings further stress the need of reliable biomarkers in AD research.

Association between EEG markers and GM changes

In the present study the relationship between an EEG marker

(the alpha3/alpha2 power ratio) and the cortical thickness in subjects with MCI was investigated. The alpha3/alpha 2 power ratio has been chosen because in previous works it has been demonstrated that MCI subjects with higher alpha 3/alpha 2 ratio are at major risk to develop AD [14,15]. Our results show that the MCI group with higher alpha3/alpha2 ratio has a greater global cortical atrophy than the other subgroups, thus confirming a large body of literature [6,49,50]. Furthermore, the greater atrophy is significant in two specific brain areas: precuneus and supramarginal gyrus (a brain area belonging to the inferior parietal lobule), both in left and right hemisphere. These results were largely expected considering previous studies. Indeed, structural and functional abnormalities of the precuneus were observed in MCI [50-53] as well as in Alzheimer's disease [54,55] so that the atrophy of precuneus has been considered as a pathognomonic marker of early AD. Moreover, in the present study, there is a very interesting result. The atrophy of precuneus is coupled with the atrophy in supramarginal gyrus and, at lesser extent, with inferior parietal, insula and superior temporal gyrus. This atrophy pattern is clearly expressed in the group of MCI subjects with higher alpha3/alpha2 power ratio. The authors found that there is a preferential pathway of connectivity of the dorsal precuneus with supramarginal gyrus, parietal cortex, superior temporal gyrus and insula. As a consequence, the atrophy we detected in the MCI group with higher alpha3/alpha2 ratio power could be hypothesized as the loss of GM in an entire anatomo-functional network more than atrophy of isolated brain areas. Of note, it is widely accepted that AD is the result of a cortical network impairment more than the atrophy of single cortical areas [56,57]. In subjects with low or middle alpha3/alpha2 power ratio the cognitive impairment is possibly due to cerebrovascular impairment or non-AD degenerative process. Although the rigid selection criteria adopted to include in the study patients with

primary cognitive deficits, in the clinical practice is not infrequent to have MCI subjects not due to AD [56-59].

Neurophysiological and clinical implications

Klimesch and coworkers have convincingly demonstrated that the upper alpha band (~10–13 Hz) specifically reflects encoding memory processes [60,30]. Recent EEG and magnetoencefalography (MEG) studies have confirmed that a correct functioning of memory, both in encoding and in retrieval, requires the high alpha rhythm desynchronization (or power decrease; [61-67]. From a neurophysiological point of view the synchronization (or power increase) of EEG alpha power has been associated with the inhibition timing hypothesis [18] and with poor information transmission, according to the entropy's theory [20,68]. The increases in alpha amplitudes reflect inhibition of cortical brain regions [18,69]. Similarly, the entropy's theory stated that synchronization is disadvantageous for storing information, as it reduces the flow of information [20]. Entropy is a measure of the richness of information encoded in a sequence of events. Applying this concept to the neural networks, it has been demonstrated [70] that the degree of information that is encoded in neural assemblies increases as a function of desynchronization and decreases as a function of synchronized firing patterns [71,72]. This hypothesis has been confirmed in clinical studies in patients with memory deficits [73] as well as during states where there is little cognitive processing (e.g., epileptic seizures or slow wave sleep; [70,74,75]. As regards cognitive impairment due to AD, the typical synaptic loss could prevent the physiological flexibility of brain neural assemblies, impeding the desynchronizing downstream modulation of the brain activity. As a consequence, it could be hypothesized that the disruption of cortical network due to degenerative disease, inducing cortical atrophy, could determine an over synchronization of the brain oscillatory activity. The synchronization state of the high alpha power could prevent the creation of a semantic sensory code and, consequently, of the episodic memory trace [76,77]. In previous seminal studies, high alpha frequency has been specifically related to semantic memory processes [74,87,1]. Of note, in subjects with early cognitive decline, the impairment of the semantic features of memory has been recently accepted as a hallmark for the early AD diagnosis [1,2]. Indeed, according to the new diagnostic criteria of AD, the measurement of sensitivity to semantic cueing can successfully differentiate patients with AD from healthy controls, even when patients are equated to controls on MMSE scores or when disease severity is very mild. Our results are generally in line with this hypothesis, suggesting that increase in power of high alpha brain oscillations reflects a block of information processes. However, the present study goes one step further, linking the increase of high alpha synchronization to the atrophy of a specific brain network, correlated with impairment in memory performances.

Increase of alpha3/alpha2 EEG power ratio and the default mode network (DMN)

Several fMRI studies of AD patients have demonstrated alterations of the DMN [1,79-83]. Previous studies also showed that in AD patients a decreased DMN functional connectivity is coupled with an increased prefrontal connectivity [82,83]. A recent resting state fMRI study suggested that regions of enhanced connectivity in AD are part of the salience network [78,84]. Recent findings in fMRI studies suggest that the pathophysiological process of AD exerts specific deleterious effects on distributed memory circuits, even prior to clinical manifestations of significant memory impairment. In particular, the disruption of the intrinsic connectivity of these networks is observable even during the resting state in asymptomatic individuals with early AD who have

high amyloid burden both in the medial temporal lobe (MTL) system and the set of cortical regions collectively referred to as the default network [85,86]. Specific regions of the default network, namely the precuneus and posterior cingulate, are selectively vulnerable to early amyloid deposition in AD pathology. These regions are also thought to play a key role in both memory encoding and retrieval, and are strongly functionally connected to the MTL. Recent studies have demonstrated that during the successful encoding of new items there is a desynchronization in the temporo-parietal memory-related networks whereas a synchronization prevent a successful semantic encoding [87,88]. It is of great interest that there is an overlapping between the brain regions associated with increase of EEG alpha3/alpha2 power ratio (hypersynchronization of high alpha) in our study and the DMN nodes in fMRI studies related to memory encoding [86-88]. The deleterious role of synchronization has been recently demonstrated by an interesting study facing the intriguing relationship between the functional and structural degeneration of DMN in AD [85]. The authors detected some hub regions (eteromodal associative regions) typical of the DMN. These regions were demonstrated to be selectively vulnerable in AD pathology, due to the damage of inhibitory interneurons providing a loss of inhibition at cellular level. According to the authors, the disinhibition provokes an increasing amount of neural activity at network level, giving as a final result an hyper synchronization of brain areas. Of note, this over activity is excitotoxic and determines cellular apoptosis and brain atrophy. Our results are in line with these previous influential studies. A possible integrative view of all the results could be as follows: 1) the higher neuronal activity in the hub regions starts from a dysfunction of cellular inhibition; 2) the consequent disinhibition drives neural network to an over synchronization; 3) this over synchronization is peculiar of the hub regions of the DMN; 4) these over activated regions are prone ot degeneration and atrophy ; 5) a possible neurophysiologic sign of this over synchronization is the increase of the alpha3/alpha 2 power ratio we have found in typical hub regions [89,90].

Conclusion

The present results show that that synchronization (or increase in power) of high alpha is associated with greater cortical atrophy. The greater cortical atrophy is present both considering the whole brain volume and in a peculiar memory-related network, including precuneus and temporo-parietal cortices. The combination of EEG alpha3/alpha2 ratio and cortical thickness measure could be useful for identifying individuals at risk for progression to AD dementia and may be of value in clinical context.

References

1. Dubois B, Feldman HH, Jacova C, Dekosky ST, Barberger-Gateau P, et al. (2007) Research criteria for the diagnosis of Alzheimer's disease: revising the NINCDS-ADRDA criteria. *Lancet Neurol*. 6: 734-46. Review.
2. Albert MS, DeKosky ST, Dickson D, Dubois B, Feldman HH, et al. (2011) Phelps CH. The diagnosis of mild cognitive impairment due to Alzheimer's disease: recommendations from the National Institute on Aging-Alzheimer's Association workgroups on diagnostic guidelines for Alzheimer's disease *Alzheimers Dement*. 7: 270-279.
3. Hampel H, Bürger K, Teipel SJ, Bokde AL, Zetterberg H, et al. (2008) Core candidate neurochemical and imaging biomarkers of Alzheimer's disease. *Alzheimers Dement* 4: 38-48.
4. Galluzzi S, Geroldi C, Amicucci G, Bocchio-Chiavetto L, Bonetti M, et al. (2013) Supporting evidence for using biomarkers in the diagnosis of MCI due to AD. *J Neurol* 260: 640-650.
5. Frisoni GB, Sabattoli F, Lee AD, Dutton RA, Toga AW, et al. (2006) In vivo neuropathology of the hippocampal formation in AD: a radial mapping MR-based study. *Neuroimage* 32: 104-110.

6. Frisoni GB, Pievani M, Testa C, Sabattoli F, Bresciani L, et al. (2007) The topography of grey matter involvement in early and late onset Alzheimer's disease. *Brain* 130: 720-730.
7. Frisoni GB, Ganzola R, Canu E, Rüb U, Pizzini FB, et al. (2008) Mapping local hippocampal changes in Alzheimer's disease and normal ageing with MRI at 3 Tesla. *Brain* 131: 3266-3276.
8. Frisoni GB, Prestia A, Rasser PE, Bonetti M, Thompson PM (2009) In vivo mapping of incremental cortical atrophy from incipient to overt Alzheimer's disease. *J Neurol* 256: 916-924.
9. van Strien NM, Cappaert NL, Witter MP (2009) The anatomy of memory: an interactive overview of the parahippocampal-hippocampal network. *Nat Rev Neurosci* 10: 272-282.
10. Missonnier P, Herrmann FR, Michon A, Fazio-Costa L, Gold G, et al. (2010) Early disturbances of gamma band dynamics in mild cognitive impairment. *J Neural Transm* 117: 489-498.
11. Steriade M (2006) Grouping of brain rhythms in corticothalamic systems. *Neuroscience* 137: 1087-1106.
12. Moretti DV, Pievani M, Geroldi C, Binetti G, Zanetti O, et al. (2009a) Increasing hippocampal atrophy and cerebrovascular damage is differently associated with functional cortical coupling in MCI patients. *Alzheimer Dis Assoc Disord* 23: 323-332.
13. Moretti DV, Pievani M, Fracassi C, Binetti G, Rosini S, et al. (2009b) Increase of theta/gamma and alpha3/alpha2 ratio is associated with amygdalo-hippocampal complex atrophy. *J Alzheimer Disease*, 120: 295-303.
14. Moretti DV, Frisoni GB, Fracassi C, Pievani M, Geroldi C, et al. (2011) MCI patients' EEGs show group differences between those who progress and those who do not progress to AD. *Neurobiol Aging* 32: 563-571.
15. Moretti DV, Prestia A, Fracassi C, Binetti G, Zanetti O, et al. (2012) Specific EEG changes associated with atrophy of hippocampus in subjects with mild cognitive impairment and Alzheimer's disease. *Int J Alzheimers Dis* 2012: 253153.
16. Bakkour A, Morris JC, Dickerson BC (2009) The cortical signature of prodromal AD: regional thinning predicts mild AD dementia. *Neurology* 72: 1048-1055.
17. Klimesch W, Doppelmayr M, Hanslmayr S (2006) Upper alpha ERD and absolute power: their meaning for memory performance. *Prog Brain Res* 159: 151-165.
18. Klimesch W, Sauseng P, Hanslmayr S (2007) EEG alpha oscillations: the inhibition-timing hypothesis. *Brain Res Rev* 53: 63-88.
19. Klimesch W (2011) Evoked alpha and early access to the knowledge system: the P1 inhibition timing hypothesis. *Brain Res* 1408: 52-71.
20. Shannon CE, Weaver W (1949) *The Mathematical Theory of Communication*. Urbana, IL: University of Illinois Press.
21. Folstein MF, Folstein SE, McHugh PR (1975). 'Mini mental state': a practical method for grading the cognitive state of patients for clinician. *J Psychiatr Res* 12: 189-98.
22. Hughes CP, Berg L, Danziger WL, Coben LA, Martin RL (1982) A new clinical scale for the staging of dementia. *Br J Psychiatry* 140: 566-572.
23. Rosen WG, Terry RD, Fuld PA, Katzman R, Peck A (1980) Pathological verification of ischemic score in differentiation of dementias. *Ann Neurol* 7: 486-488.
24. Lawton MP, Brody EM (1969) Assessment of older people: self-maintaining and instrumental activities of daily living. *Gerontologist* 9: 179-186.
25. Petersen RC, Doody R, Kurz A, Mohs RC, Morris JC, et al. (2001) Current concepts in mild cognitive impairment. *Arch Neurol* 58: 1985-1992.
26. Portet F, Ousset P J, Visser P J, Frisoni G B, Nobili F et al. (2006) and the MCI Working Group of the European Consortium on Alzheimer's Disease (EADC). Mild cognitive impairment (MCI) in medical practice: a critical review of the concept and new diagnostic procedure. Report of the MCI Working Group of the European Consortium on Alzheimer's disease. *J. Neurol. Neurosurg. Psychiatry*; 77: 714-718.
27. Lezak M, Howieson D, Loring, DW (2004) *Neuropsychological Assessment*, fourth edition. Oxford: University Press.
28. Radloff LS (1977) The CES-D scale: A self-report depression scale for research in the general population. *Applied Psychological Measurement* 1:385-401.
29. Moretti DV, Babiloni F, Carducci F, Cincotti F, Remondini E, et al. (2003) Computerized processing of EEG-EOG-EMG artifacts for multi-centric studies in EEG oscillations and event-related potentials. *Int J Psychophysiol* 47: 199-216.
30. Klimesch W (1997) EEG-alpha rhythms and memory processes. *Int J Psychophysiol* 26: 319-340.
31. Klimesch W (1999) EEG alpha and theta oscillations reflect cognitive and memory performance: a review and analysis. *Brain Res Brain Res Rev* 29: 169-195.
32. Moretti DV, Babiloni C, Binetti G, Cassetta E, Dal Forno G, et al. (2004) Individual analysis of EEG frequency and band power in mild Alzheimer's disease. *Clin Neurophysiol* 115: 299-308.
33. Moretti DV, Miniussi C, Frisoni G, Zanetti O, Binetti G, et al. (2007a) Vascular damage and EEG markers in subjects with mild cognitive impairment. *Clinical neurophysiology*. 118: 1866-1876.
34. Moretti DV, Pievani M, Fracassi C, Geroldi C, Calabria M, et al. (2008) Brain vascular damage of cholinergic pathways and EEG markers in mild cognitive impairment. *J Alzheimers Dis* 15: 357-372.
35. Fischl B, Sereno MI, Dale AM (1999) Cortical surface-based analysis. II: Inflation, flattening, and a surface-based coordinate system. *Neuroimage* 9: 195-207.
36. Dale AM, Fischl B, Sereno MI (1999) Cortical surface-based analysis. I. Segmentation and surface reconstruction. *Neuroimage* 9: 179-194.
37. Ségonne F, Dale AM, Busa E, Glessner M, Salat D et al. (2004). A hybrid approach to the skull stripping problem in MRI. *Neuroimage*. 22:1060-1075.
38. Fischl B, Dale AM (2000) Measuring the thickness of the human cerebral cortex using magnetic resonance images *Proc Natl Acad Sci U S A* 97:11050-11055.
39. Han X, Jovicich J, Salat D, van der Kouwe A, Quinn B, et al. (2006) Reliability of MRI-derived measurements of human cerebral cortical thickness: the effects of field strength, scanner upgrade and manufacturer. *Neuroimage* 32: 180-194.
40. Gronenschild EH, Habets P, Jacobs HI, Mengelers R, Rozendaal N, et al. (2012) The effects of FreeSurfer version, workstation type, and Macintosh operating system version on anatomical volume and cortical thickness measurements. *PLoS One* 7: e38234.
41. Kuperberg GR, Broome MR, McGuire PK, David AS, Eddy M, et al. (2003) Regionally localized thinning of the cerebral cortex in schizophrenia. *Arch Gen Psychiatry* 60: 878-888.
42. Rosas HD, Liu AK, Hersch S, Glessner M, Ferrante RJ, et al. (2002) Regional and progressive thinning of the cortical ribbon in Huntington's disease. *Neurology* 58: 695-701.
43. DeCarli C, Fletcher E, Ramey V, Harvey D, Jagust WJ (2005) Anatomical mapping of white matter hyperintensities (WMH): exploring the relationships between periventricular WMH, deep WMH, and total WMH burden. *Stroke* 36: 50-55.
44. Pannanen C, Testa C, Laasko MP, Hallikainen M, Helkala E L et al. (2005). A voxel based morphometry study on mild cognitive impairment. *J Neurol Neurosurg Psychiatry* 76:11-14.
45. Markesbery WR, Schmitt FA, Kryscio RJ, Davis DG, Smith CD, et al. (2006) Neuropathologic substrate of mild cognitive impairment. *Arch Neurol* 63: 38-46.
46. McKhann GM, Knopman DS, Chertkow H, Hyman BT, Jack CR Jr, et al. (2011) The diagnosis of dementia due to Alzheimer's disease: recommendations from the National Institute on Aging-Alzheimer's Association workgroups on diagnostic guidelines for Alzheimer's disease. *Alzheimers Dement* 7: 263-269.
47. Sperling RA, Aisen PS, Beckett LA, Bennett DA, Craft S, et al. (2011) Toward defining the preclinical stages of Alzheimer's disease: recommendations from the National Institute on Aging-Alzheimer's Association workgroups on diagnostic guidelines for Alzheimer's disease. *Alzheimers Dement* 7:280-292.
48. Galluzzi S, Geroldi C, Amicucci G, Bocchio-Chiavetto L, Bonetti M, et al. (2012) Translational Outpatient Memory Clinic Working. Supporting evidence for using biomarkers in the diagnosis of MCI due to AD. *Group. J Neurol* 260: 640-650.
49. Frisoni GB (2012) Alzheimer disease: biomarker trajectories across stages of Alzheimer disease. *Nat Rev Neurol* 8: 299-300.
50. Dai W, Lopez OL, Carmichael OT, Becker JT, Kuller LH, et al. (2009) Mild cognitive impairment and alzheimer disease: patterns of altered cerebral blood flow at MR imaging. *Radiology* 250: 856-866.

51. Matsuda H (2007) The role of neuroimaging in mild cognitive impairment. *Neuropathology* 27: 570-577.
52. Petrella JR, Wang L, Krishnan S, Slavin MJ, Prince SE, et al. (2007) Cortical deactivation in mild cognitive impairment: high-field-strength functional MR imaging. *Radiology* 245: 224-235.
53. Pihlajamäki M, Jauhiainen AM, Soininen H (2009) Structural and functional MRI in mild cognitive impairment. *Curr Alzheimer Res* 6: 179-185.
54. Sperling RA, Dickerson BC, Pihlajamäki M, Vannini P, LaViolette PS, et al. (2010) Functional alterations in memory networks in early Alzheimer's disease. *Neuromolecular Med* 12: 27-43.
55. Ryu SY, Kwon MJ, Lee SB, Yang DW, Kim TW, et al. (2010) Measurement of precuneal and hippocampal volumes using magnetic resonance volumetry in Alzheimer's disease. *J Clin Neurol* 6: 196-203.
56. Ghaem O, Mellet E, Crivello F, Tzourio N, Mazoyer B, et al. (1997) Mental navigation along memorized routes activates the hippocampus, precuneus, and insula. *Neuroreport* 8: 739-744.
57. Leichnetz GR (2001) Connections of the medial posterior parietal cortex (area 7m) in the monkey. *Anat Rec* 263: 215-236.
58. Cavanna AE, Trimble MR (2006) The precuneus: a review of its functional anatomy and behavioural correlates. *Brain* 129: 564-583.
59. Wenderoth N, Debaere F, Snaert S, Swinnen SP (2005) The role of anterior cingulate cortex and precuneus in the coordination of motor behaviour. *Eur J Neurosci* 22: 235-246.
60. Klimesch W, Schimke H, Doppelmayr M, Ripper B, Schwaiger J, et al. (1996) Event-related desynchronization (ERD) and the Dm effect: does alpha desynchronization during encoding predict later recall performance? *Int J Psychophysiol* 24: 47-60.
61. Klimesch W, Doppelmayr M, Stadler W, Pöllhuber D, Sauseng P, et al. (2001) Episodic retrieval is reflected by a process specific increase in human electroencephalographic theta activity. *Neurosci Lett* 302: 49-52.
62. Fries P, Reynolds JH, Rorie AE, Desimone R (2001) Modulation of oscillatory neuronal synchronization by selective visual attention. *Science* 291: 1560-1563.
63. Kilner JM, Mattout J, Henson R, Friston KJ (2005) Hemodynamic correlates of EEG: a heuristic. *Neuroimage* 28: 280-286.
64. Wyart V, Tallon-Baudry C (2008) Neural dissociation between visual awareness and spatial attention. *J Neurosci* 28: 2667-2679.
65. Spitzer B, Hanslmayr S, Opitz B, Mecklinger A, Bäuml KH (2009) Oscillatory correlates of retrieval-induced forgetting in recognition memory. *J Cogn Neurosci* 21: 976-990.
66. Staudigl T, Hanslmayr S, Bäuml KH (2010) Theta oscillations reflect the dynamics of interference in episodic memory retrieval. *J Neurosci* 30: 11356-11362.
67. Hanslmayr S, Spitzer B, Bäuml KH (2009) Brain oscillations dissociate between semantic and nonsemantic encoding of episodic memories. *Cereb Cortex* 19: 1631-1640.
68. Hanslmayr S, Staudigl T, Fellner MC (2012) Oscillatory power decreases and long-term memory: the information via desynchronization hypothesis. *Front Hum Neurosci* 6: 74.
69. Jensen O, Mazaheri A (2010) Shaping functional architecture by oscillatory alpha activity: gating by inhibition. *Front Hum Neurosci* 4: 186.
70. Zhang S, Li CS (2012) Functional connectivity mapping of the human precuneus by resting state fMRI. *Neuroimage* 59: 3548-3562.
71. Norman KA (2010) How hippocampus and cortex contribute to recognition memory: revisiting the complementary learning systems model. *Hippocampus* 20: 1217-1227.
72. Schneidman E, Puchalla JL, Segev R, Harris RA, Bialek W, et al. (2011) Synergy from silence in a combinatorial neural code. *J Neurosci* 31: 15732-15741.
73. Kurimoto R, Ishii R, Canuet L, Ikezawa K, Iwase M, et al. (2012) Induced oscillatory responses during the Sternberg's visual memory task in patients with Alzheimer's disease and mild cognitive impairment. *Neuroimage* 59: 4132-4140.
74. Goard M, Dan Y (2009) Basal forebrain activation enhances cortical coding of natural scenes. *Nat Neurosci* 12: 1444-1449.
75. Chalk M, Herrero JL, Gieselmann MA, Delicato LS, Gotthardt S, et al. (2010) Attention reduces stimulus-driven gamma frequency oscillations and spike field coherence in V1. *Neuron* 66: 114-125.
76. Barlow HB (1961) "The coding of sensory messages," in *Current Problems in Animal Behaviour* 331-360.
77. Bialek W, Rieke F, de Ruyter van Steveninck RR, Warland D (1991) Reading a neural code. *Science* 252: 1854-1857.
78. Craik FI (2002) Levels of processing: past, present, and future? *Memory* 10: 305-318.
79. Allen G, Barnard H, McColl R, Hester AL, Fields JA, et al. (2007) Reduced hippocampal functional connectivity in Alzheimer disease. *Arch Neurol* 64: 1482-1487.
80. Greicius MD, Srivastava G, Reiss AL, Menon V (2004) Default-mode network activity distinguishes Alzheimer's disease from healthy aging: evidence from functional MRI. *Proc Natl Acad Sci U S A* 101: 4637-4642.
81. Li SJ, Li Z, Wu G, Zhang MJ, Franczak M, et al. (2002) Alzheimer Disease: evaluation of a functional MR imaging index as a marker. *Radiology* 225: 253-259.
82. Rombouts SA, Barkhof F, Goekoop R, Stam CJ, Scheltens P (2005) Altered resting state networks in mild cognitive impairment and mild Alzheimer's disease: an fMRI study. *Hum Brain Mapp* 26: 231-239.
83. Wang K, Liang M, Wang L, Tian L, Zhang X, et al. (2007) Altered functional connectivity in early Alzheimer's disease: a resting-state fMRI study. *Hum Brain Mapp* 28: 967-978.
84. Zhou J, Greicius MD, Gennatas ED, Growdon ME, Jang JY, et al. (2010) Divergent network connectivity changes in behavioural variant frontotemporal dementia and Alzheimer's disease. *Brain* 133: 1352-1367.
85. Agosta F, Pievani M, Geroldi C, Copetti M, Frisoni GB, et al. (2012) Resting state fMRI in Alzheimer's disease: beyond the default mode network. *Neurobiol Aging* 33: 1564-1578.
86. de Haan W, Mott K, van Straaten EC, Scheltens P, Stam CJ (2012) Activity dependent degeneration explains hub vulnerability in Alzheimer's disease. *PLoS Comput Biol* 8: e1002582.
87. Pievani M, de Haan W, Wu T, Seeley WW, Frisoni GB (2011) Functional network disruption in the degenerative dementias. *Lancet Neurol* 10: 829-843.
88. Jones DT, Machulda MM, Vemuri P, McDade EM, Zeng G, et al. (2011) Age-related changes in the default mode network are more advanced in Alzheimer disease. *Neurology* 77: 1524-1531.
89. Brier MR, Thomas JB, Snyder AZ, Benzinger TL, Zhang D, et al. (2012) Loss of intranetwork and internetwork resting state functional connections with Alzheimer's disease progression. *J Neurosci* 32: 8890-8899.
90. Bhattacharya BS, Coyle D, Maguire LP (2011) Alpha and theta rhythm abnormality in Alzheimer's Disease: a study using a computational model. *Adv Exp Med Biol* 718: 57-73.